Article:
Kluzek, M, Tyler, AII orcid.org/0000-0003-2116-1084, Wang, S et al. (5 more authors) (2017) Influence of a pH-sensitive polymer on the structure of monoolein cubosomes. Soft Matter, 41. pp. 7571-7577. ISSN 1744-683X

https://doi.org/10.1039/C7SM01620D

Soft Matter

Accepted Manuscript

This article can be cited before page numbers have been issued, to do this please use: M. Kluzek, A. I.I. Tyler, S. Wang, R. Chen, C. Marques, F. Thalmann, J. Seddon and M. Schmutz, *Soft Matter*, 2017, DOI: 10.1039/C7SM01620D.

This is an Accepted Manuscript, which has been through the Royal Society of Chemistry peer review process and has been accepted for publication.

Accepted Manuscripts are published online shortly after acceptance, before technical editing, formatting and proof reading. Using this free service, authors can make their results available to the community, in citable form, before we publish the edited article. We will replace this Accepted Manuscript with the edited and formatted Advance Article as soon as it is available.

You can find more information about Accepted Manuscripts in the author guidelines.

Please note that technical editing may introduce minor changes to the text and/or graphics, which may alter content. The journal's standard Terms & Conditions and the ethical guidelines, outlined in our author and reviewer resource centre, still apply. In no event shall the Royal Society of Chemistry be held responsible for any errors or omissions in this Accepted Manuscript or any consequences arising from the use of any information it contains.

ROYAL SOCIETY OF CHEMISTRY

rsc.li/soft-matter-journal

View Article Online
DOI: 10.1039/C7SM01620D
ROYAL SOCIETY OF CHEMISTRY

Journal Name

ARTICLE TYPE

Cite this: DOI: 10.1039/xxxxxxxxxx

Influence of a pH-sensitive polymer on the structure of monoolein cubosomes

Monika Kluzek,*[a] Arwen I.I. Tyler,[b,c] Shiqi Wang,[d] Rongjun Chen,[d] Carlos M. Marques,[a] Fabrice Thalmann,*[a] John M. Seddon,[b] and Marc Schmutz[a]

Received Date
Accepted Date

DOI: 10.1039/xxxxxxxxxx

www.rsc.org/journalname

Cubosomes consist in submicron size particles of lipid bicontinuous cubic phases stabilized by surfactant polymers. They provide an appealing road towards the practical use of lipid cubic phases for pharmaceuticals and cosmetics applications, and efforts are currently being made to control the encapsulation and release properties of these colloidal objects. We overcome in this work the lack of sensitivity of monoolein cubosomes to pH conditions by using a pH sensitive polymer designed to strongly interact with the lipid structure at low pH. Our cryo-transmission electron microscope (Cryo-TEM) and small-angle X-ray scattering (SAXS) results show that in the presence of the polymer the cubic phase structure is preserved at neutral pH, albeit with a larger cell size. At pH 5.5, in the presence of the polymer, the nanostructure of the cubosome particles is significantly altered, providing a pathway to design pH-responsive cubosomes for applications in drug delivery.

1 Introduction

Since the pioneering work of Luzzati[1,2] and Larsson[3,4] where the monoolein (MO)/water phase behaviour was studied for the first time,[5] several studies have explored the possible use of MO-based cubic phases as potential hosting matrices in pharmaceutical[6–10] and food applications.[11,12] The lipid cubic crystals have distinctive structural and chemical advantages, including highly ordered periodic structures, a large surface area of the lipid/water interface (400 m^2 g^{-1})[13], tuneable structural parameters, and provide a biocompatible platform for entrapment of proteins, peptides, and other biomolecules. A significant emphasis has been placed on cubic phases due to their polar/apolar continuous domains, which allow for the encapsulation of a broad range of hydrophilic/hydrophobic molecules[14] and for controlled release of a cargo, thus maintaining the therapeutic concentration range over a longer period of time.[7]

Cubosomes are stable nanoparticle dispersions formulated from bulk cubic phases (Fig. 1). They have been gathering increasing attention due to their potential applications in nanomedicine. However, pure MO systems alone do not respond to biological or external stimuli such as temperature, light, pH or ionic strength. Hence, significant efforts are being made towards more accurately controlled release of target biomolecules[15,16] and on modulating the release properties of the host-guest lipid cubic phases in response to specific external conditions.[17–21] This approach recently led to the development of stimuli responsive cubosome-based drug-delivery systems with the capacity of releasing their content in response to external triggers. Several authors have reported the effect of pH changes on mixtures of monoolein-charged lipid bicontinuous cubic phases[22–25]. These systems were shown to reversibly change from a cubic phase to an inverted hexagonal H_{II} or lamellar L_α phase in response to acidic (pH 2) conditions. This strategy was further exploited by Negrini

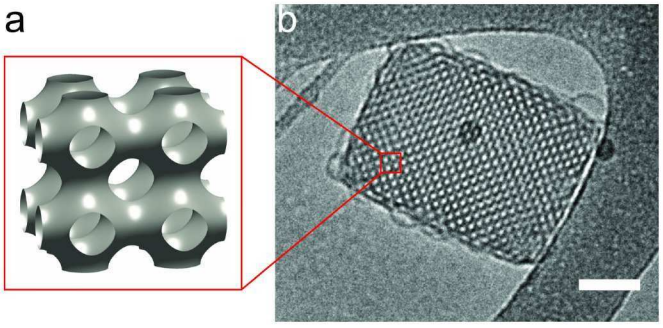

Fig. 1 a) Graphical picture of an inverse cubic phase with primitive type structure *Im3m*, b) Cryo-TEM image of a monoolein cubosome stabilized with 5 wt % Pluronic F127. Scale bar, 100 nm.

[a] *Université de Strasbourg, CNRS, Institut Charles Sadron, UPR022, 23 rue du Loess, 67034 Strasbourg Cedex, France; E-mails: monika.kluzek@ics-cnrs.unistra.fr, fabrice.thalmann@ics-cnrs.unistra.fr*
[b] *Department of Chemistry, Imperial College London, South Kensington Campus, London SW7 2AZ, U.K.*
[c] *Food Colloids and Processing Group, School of Food Science and Nutrition, University of Leeds, Leeds LS2 9JT, U.K.*
[d] *Department of Chemical Engineering, Imperial College London, South Kensington Campus, London SW7 2AZ, U.K.*

View Article Online
DOI: 10.1039/C7SM01620D

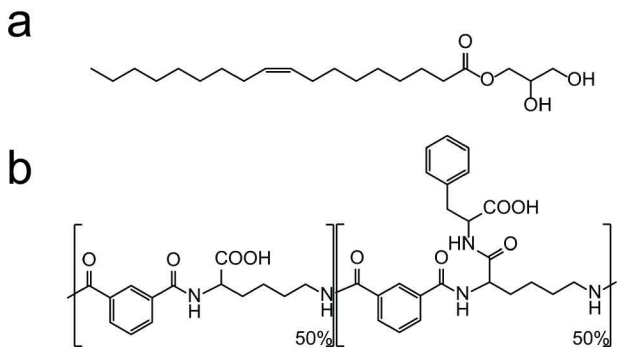

Fig. 2 The chemical structures of a) Monoolein (MO) and b) Poly(L-lysine-*iso*-phthalamide) chain grafted with phenylalanine (PP50).

et al.[21] who presented a pH-responsive cubic phase, where controlled release of cargo is achieved by adapted host-guest electrostatic interactions.

In this work, we describe a new MO-based pH-sensitive cubosome system we have developed, loaded with a pH-sensitive polymer (see Fig. 2 a). This polymer, a poly (L-lysine-*iso*-phthalamide) grafted with L-phenylalanine at the degree of grafting of 50% hereafter referred as PP50, is a promising pseudopeptidic polymer whose hydrophilic/hydrophobic balance depends on external pH.[26–30] It is by design capable of mimicking the activity of membrane-penetrating peptides. The presence of carboxylic acid side groups causes reversible conformational changes in an aqueous environment from extended charged polyelectrolyte chains at neutral pH, to a globular state at acidic pH, resulting in a higher binding affinity for the lipid membrane, causing its subsequent disruption. Thus, PP50 is an appealing example of a stimulus-responsive material, potentially able to minimise drug losses at neutral pH while conversely triggering rapid intracellular drug release from the cubic phase in an acidic environment.

In this work, we describe how the pseudopeptide PP50 can be associated with standard MO cubosomes prepared by sonication and stabilization with the nonionic Pluronic F127 surfactant.[31] We have studied the structure of MO cubosomes incorporating a small amount (10 wt %) of PP50 at two distinct pH values: pH 7.5 and pH 5.5. The crystallographic structure and the cubic cell size were determined by by SAXS, whilst the morphology and topology of the MO-cubosomes were characterised by Cryo-TEM.

It was found that under neutral pH conditions, the presence of polymer preserves the original *Im3m* cubosome structure, while a significant amount of structural disruption, with a partial disappearance of the cubic phase, is observed under acidic conditions. This suggests that our novel system has a strong potential for developing pH-responsive encapsulation vectors based on cubosomes.

2 Experimental

Materials

Monoolein powder (1-Oleoyl-rac-glycerol, C18:1c9, M_w = 356.54 Da), Pluronic F127 (PEO_{99}-PPO_{67}-PEO_{99}, M_w = 12600 Da) and buffer components (HEPES, Citrate buffer) were supplied by Sigma-Aldrich, Co. (Saint-Quentin, France). All chemicals had purities of >98% and were used without further purification.

Polymer synthesis and characterisation

The polymer PP50 was synthesised as described previously.[32] Briefly, the parent polymer PLP (poly(L-lysine-*iso*-phthalamide)) was synthesized by polycondensation of L-lysine methyl ester dihydrochloride and *iso*-phthaloyl chloride followed by ester hydrolysis. After purification, PLP was conjugated with L-phenylalanine methyl ester hydrochloride by DCC-coupling reaction followed by ester hydrolysis. The final PP50 was obtained after dialysis using a Visking membrane tubing (molecular weight cut-off, 12000-14000 Da). PP50 is a linear copolymer, composed of a sequence of 50% unsubstituted and 50% phenylalanine substituted L-lysine *iso*-phthalamide monomers (see Fig. 2 b). The polymers used in the present study had a number averaged molecular weight M_n = 23.0 kDa, and a mass averaged molecular weight M_w = 45.8 kDa, as determined using an aqueous gel permeation chromatography (GPC) system (Viscotek, UK). The polymer is a weak acid polyelectrolyte, with an estimated ionization constant $pK_a \sim 6.5$.

Sample preparation

Colloidal dispersions of cubosomes were prepared as described by Landh.[33] Briefly, for each sample, 50 mg of pure lipid was dispersed in chloroform, and the organic solvent removed under a nitrogen stream followed by overnight vacuum pumping.

SAXS samples: The lipid deposit was hydrated with 94 wt % buffer solution (0.707 mL), and then subjected to 10 freeze-thaw cycles. The resulting lipid dispersion was a cubic phase in excess water (*Pn3m*, characterisation not shown). Following the freeze-thaw cycles, a Pluronic F127 aqueous solution was added (2.68 mg surfactant in 0.30 mL buffer) for the polymer free reference samples, while Pluronic F127 (2.68 mg) dispersed with PP50 (4.84 mg) in 0.294 mL of buffer solution, was added for polymer loaded samples, corresponding to a total volume of 1 mL of buffer.

Cryo-TEM samples: The preparation followed similar steps to the preparation of the X-ray samples, but using larger volumes of buffer. The lipid deposit was first hydrated with a buffer solution (1.288 mL), followed by 10 freeze-thaw cycles, and 2.68 mg of Pluronic F127 and 4.84 mg of PP50 polymer dispersed in 1.288 mL of buffer (2.576 mL total volume of a buffer) were added.

Samples were probe-sonicated (Bioblock VibraCell 72412) at 30% amplitude for 5 min total time at 1 on/off cycle period to prevent overheating. The two hydration solutions used in the study were set to pH 7.5 with HEPES buffer (20 mM) and to pH 5.5 with citrate buffer (100 mM) prior to mixing with lipids. Hydration, sonication and stabilisation with the surfactants transformed the bicontinuous cubic phase into cubosome dispersions. Samples were then characterised by SAXS or Cryo-TEM. Cryo-TEM imaging was performed with fresh samples (a couple of hours) while SAXS samples had to be prepared a day before being placed in the Synchrotron beam.

View Article Online
DOI: 10.1039/C7SM01620D

Cryo-TEM

A laboratory-built humidity-controlled vitrification system was used to prepare the samples for Cryo-TEM. Humidity was kept close to 80% for all experiments and the temperature was set at 22°C. A 5 μL of the sample was placed onto a grid covered by the lacey carbon film (Ted Pella), which was rendered hydrophilic via glow discharge (Elmo, Cordouan Technologies). Excess sample was removed by blotting with filter paper and the sample grid was vitrified by rapid plunging into liquid ethane (-180°C). The grids were kept in liquid nitrogen before being transferred into a Gatan 626 Cryo-holder. Cryo-TEM imaging was performed on an FEI Tecnai G2 TEM (200 kV) under low dose conditions with an Eagle slow scan CCD camera.

Cryo-TEM Image Analysis

Fast Fourier transform and sizing of the nanoparticles were performed using ImageJ software (NIH, USA) software. The error in the determination of the lattice parameter from Cryo-TEM images analysis was estimated at $\pm$ 5%.

SAXS

The cubosome structures were determined by small-angle X-ray scattering using beamline I22 at Diamond Light Source (DLS) with X-ray wavelengths of 0.73 Å. The 2-D powder diffraction pattern was recorded on an image-intensified Pilatus 2M detector. Silver behenate (a = 58.38 Å) was used to calibrate the small angle X-ray diffraction data for all measurements. SAXS data were analysed using the IDL-based AXcess software package, developed at Imperial College London. Details of the use of AXcess for data analysis can be found in ref.[34]

Dynamic Light Scattering (DLS)

The size and ζ-potential of the lipid nanoparticles were measured with a ZetaSizer Nano ZS (Malvern Instruments, UK) at 25°C. Triplicate measurements with a minimum of 10 runs were performed for each sample.

3 Results and discussion

Effect of the addition of polymer on the nanoparticle size

Prior to structural analysis, cubosomes with and without polymer and the polymer solution (3 mg mL^{-1}) were characterised in terms of particle size and ζ-potential (Table 1). As previously reported, the polymer-free cubosome particles formed stable, milky dispersions with particle sizes ranging from 170 to 220 nm under both pH conditions studied. Incorporation of 10 wt % PP50 into the cubic phase at physiological pH moderately increased the size of the nanoparticles, whilst at pH 5.5 the change was more significant (283 nm). The polydispersity index (PDI) was estimated to be in the approximate range of 0.2-0.3, for all systems studied, indicating moderately heterogeneous systems. Moreover, particle dispersions stored at room temperature over a week showed no significant changes in the size and PDI, indicating physically stable systems.

The ζ-potentials of unloaded cubosomes were -1.2 and 1.1 mV for pH 7.5 and 5.5 respectively, and only a slight decrease of these values was observed upon polymer incorporation. This points to a marginal surface coverage of the particles by the negatively charged polymers.

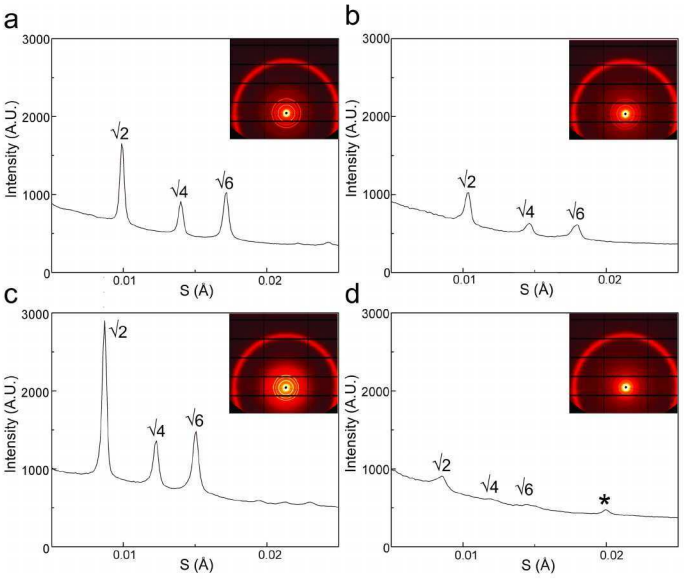

Fig. 3 1-D diffraction plots of intensity vs. scattering parameter $S=q/2\pi$ for MO-cubosomes doped with 10 wt % PP50 polymer. a) Cubosomes at pH 7.5 (lattice parameter a = 143.0 $\pm$ 0.1 Å, Peak positions: 100.8 Å, 71.4 Å, 58.2 Å); b) cubosomes at pH 5.5 (lattice parameter a = 137.3 $\pm$ 0.4 Å, Peak positions: 96.6 Å, 68.5 Å, 55.8 Å); c) cubosomes with polymer at pH 7.5 (lattice parameter a = 163.2 $\pm$ 0.1 Å, Peak positions: 114.9 Å, 81.6 Å, 66.8 Å); d) cubosomes with polymer at pH 5.5 (lattice parameter a = 167.2 $\pm$ 0.1 Å, Peak positions: 116.7 Å, 84.2 Å, 68.5 Å, 50 Å). The peak indicated by * corresponds to a spacing of 50 Å.

SAXS measurements

The liquid-crystalline structure of MO cubosomes incorporated with the polymer was investigated using SAXS. Reference samples without polymer, at pH 7.5 and 5.5 (Fig. 3a,b), showed a sequence of three well-defined diffraction peaks with relative positions at ratios of $\sqrt{2}$, $\sqrt{4}$ and $\sqrt{6}$ respectively, which corresponds to a primitive *Im3m* cubic structure. For the sample without polymer at pH 7.5, the next peaks of this space group symmetry ($\sqrt{10}$ and $\sqrt{12}$) were also visible. The corresponding lattice parameters, a = 143.0 $\pm$ 0.1 Å and a = 137.3 $\pm$ 0.4 Å for cubosomes at pH 7.5 and pH 5.5 respectively, were in agreement with previously published data.[35] The SAXS profile of the cubosomes prepared with 10 wt % of polymer at pH 7.5 (Fig. 3 c) displayed the same sequence of peaks, showing that the *Im3m* structure was preserved. The positions of the peaks indicated a lattice parameter of a = 163.2 $\pm$ 0.1 Å larger than the reference case, while the peak intensities relative to the diffuse background appeared slightly reduced (Fig. 3 and Table 2).

At lower pH (Fig. 3 d), the SAXS data of the cubosome solution incubated with PP50 polymers looked significantly more diffuse. A sequence of well visible but smaller peaks with relative positions at $\sqrt{2}$, $\sqrt{4}$ and $\sqrt{6}$ respectively was observed, still consistent with a P-type *Im3m* structure with a = 167.2 $\pm$ 0.1 Å. In addi-

View Article Online
DOI: 10.1039/C7SM01620D

Table 1 Hydrodynamic diameter and ζ-potential of cubosomes w/wo polymer and the pure PP50 solution under different pH conditions. Values are shown as averages over 3 samples with 10 runs each, and the standard deviation is used as an error estimate. As anticipated, the polymer was well dispersed at pH 7.5 and aggregated at pH 5.5 (DLS sizing data column)

Sample	Size (nm)		ζ—potential (mV)	
	pH 7.5	pH 5.5	pH 7.5	pH 5.5
Cubosomes	178.1 ± 5.2	220.9 ± 4.2	-1.2 ± 0.8	1.1 ± 0.4
Cubosomes with PP50	212.7 ± 4.7	283.3 ± 3.6	-2.1 ± 1.0	0.11 ± 0.7
PP50	N/A*	50.7 ± 4.2	-13.1 ± 2.1	-28.4 ± 1.0

* *Not enough scattering from the linear dispersed polymer chains*

** *Measured by SAXS*

*** *Obtained from Cryo-TEM images analysis of 7 cubosome nanoparticles*

Table 2 Lattice parameters (a), calculated water volume fraction (ϕ_w) and water channel radius (r_w) of MO cubosomes w/wo polymer as a function of pH

Sample	a^{**} (Å)		a^{***} (Å)		ϕ_w (%)		r_w (Å)	
	pH 7.5	pH 5.5	pH 7.5	pH 5.5	pH 7.5	pH 5.5	pH 7.5	pH 5.5
Cubosomes	143.0 ± 0.1	137.3 ± 0.4	140.2 ± 0.2	139.0 ± 0.4	44.5 ± 0.1	42.5 ± 0.1	25.8 ± 0.1	24.0 ± 0.1
Cubosomes with PP50	163.2 ± 0.1	167.2 ± 0.1	163.0 ± 0.5	156.0 ± 0.9	50.4 ± 0.1	50.4 ± 0.1	31.8 ± 0.1	33.0 ± 0.1

tion, a new peak at 50 Å (indicated by *) appeared, which was not related to the previous family of diffraction peaks.

Cryo-TEM observations

We used Cryo-TEM to visualize the nanostructure of the cubosome particles in both physiological pH 7.5 and acid pH 5.5 environments. Cryo-TEM images (Fig. 4 a,b), combined with Fast Fourier Transform (FFT) analysis, revealed that at both pHs, the reference samples formed stable bicontinuous cubic phases with an *Im3m* symmetry and a measured lattice parameter of the order of 140 Å as commonly observed in previous preparations.[36,37] This indicates that pH alone does not influence the stability of MO cubosome particles. Moreover, the bilayer thickness, as determined by image analysis, was about 36 Å (Table 2) which was in excellent agreement with values reported elsewhere.[36]

The structural symmetry of the primitive *Im3m* cubic phase was clearly preserved upon incorporation of the polymer at physiological pH (Fig. 4 c,d). More importantly, a corresponding analysis of the structural parameters showed that the presence of the polymer expanded the unit cell size a. This increase in lattice parameter was similar to what was observed in SAXS (Fig. 3 c and Table 2). From the FFT analysis of a number of selected particles, a mean lattice parameter of 160 Å was obtained.

Remarkably, in the low pH regime (5.5), where PP50 is expected to interact strongly with the lipids, some clear disruption of the underlying cubic phase structure was observed (Fig. 4e and Fig. 5). A number of changes varied from particle to particle, and within a given particle. There was in some regions a significant collapse of the structure, with disappearance of the lattice structure. FFT analysis confirmed the absence of periodicity. In other regions, the cubic regions were preserved as in the reference sample.

Finally, one could find regions in particles displaying some apparent lamellar ordering, with an anisotropic orientation confirmed by FFT analysis. Whether the cubic structure disappeared totally or only partially, our Cryo-TEM images demonstrated the pH dependent disruptive action of the polymer on the MO-bilayer within the cubic phase.

Measurements of cubic lipid phases, pure or with additives, are commonly carried out in buffer solutions of various chemical compositions, ionic strengths etc. It has been reported that such parameters, like the presence of salts of different chemical natures, the exact pH, temperature and pressure values, might all influence the phase behaviour of these lyotropic liquid crystals. In the present study, the addition of 10 wt % polymer (with respect to the lipid mass) was accompanied by a 12% increase in the value of the unit cell size (from 143 to 163 Å) in HEPES buffer (pH 7.5).

Although the polymer cannot be unambiguously located within the sample, the Cryo-TEM images and the sharp appearance of the SAXS peaks indicate that the particles were spatially homogeneous and that, if present inside, the polymer was evenly distributed. From the geometry of the primitive cubic structure, one could estimate the amount of water present in the particles compared to the bulk aqueous solution. Ignoring the Pluronic F127 and PP50, it is possible to relate the volume fraction of lipid Φ_l to the cell size a, and lipid length l in the parallel surface approximation:

$$\Phi_l = 2A_0(\frac{l}{a}) + \frac{4\pi\chi}{3}(\frac{l}{a})^3 \quad (1)$$

where A_0 and χ are respectively the ratio of the area of the minimal surface in the unit cell to the quantity (unit cell volume)$^{2/3}$, and the Euler-Poincare characteristic, which depends on the symmetry of the cubic phase.[38,39] In the case of the *Im3m* structure, the values are A_0=2.3451,and χ=-4. Using the standard monoolein value l = 18 Å in the absence of PP50 at pH 7.5 (consistent with the bilayer thickness of 36 Å seen in Cryo-TEM), one gets Φ_l= 0.555. According to this value, 50 mg of monoolein were hydrated by about 40 mg of water. The free water (1 g or more) was present in much larger amount, showing that the cubosome structures were in equilibrium with excess water. If PP50 did not penetrate the nanoparticles and was thus present only in the excess free aqueous solution, it could still act on the cubic phase indirectly, in a solvent-mediated way. An obvious mechanism would be depletion, with PP50 lowering the water chemical

View Article Online
DOI: 10.1039/C7SM01620D

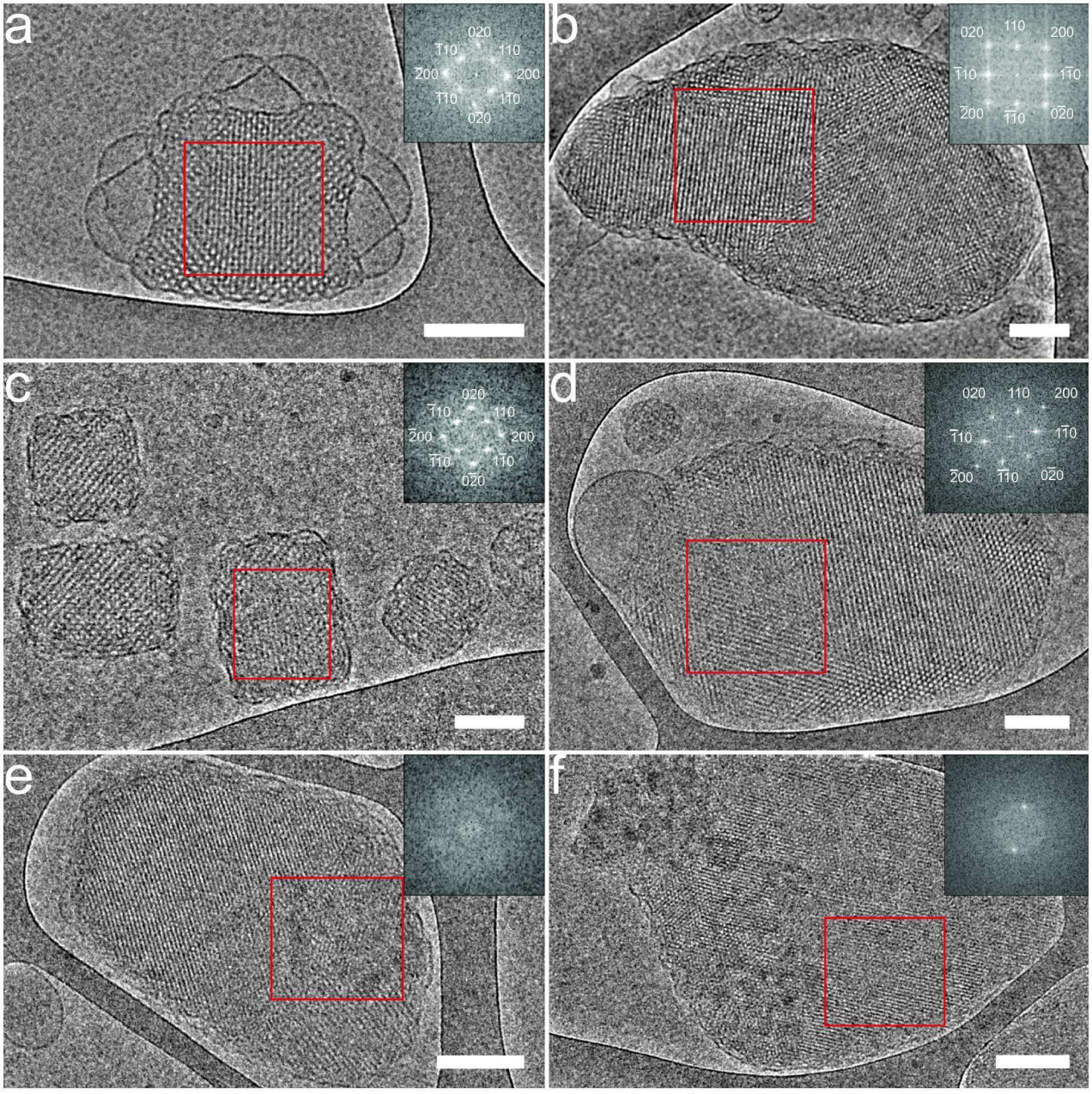

Fig. 4 Representative Cryo-TEM images of cubosome dispersions used in this study, with the corresponding Fast Fourier Transform (FFT) of red box areas (insets). Unloaded cubosome: a) pH 7.5; b) pH 5.5; c), d) cubosome/PP50 at pH 7.5. e), f) cubosomes/PP50 at pH 5.5. FFT was used for determination of the structure of the liquid crystalline particles, independently from SAXS. Scale bar, 100 nm.

View Article Online
DOI: 10.1039/C7SM01620D

potential in the excess solvent region. One would expect to see in this situation a dehydration of the lipid phase, and some decrease in the lattice size, which was contrary to our present observations. With the PP50 being deprotonated at pH 7.5, its adsorption onto the cubosome particles' outer surface should confer them with a negative surface charge, with a correspondingly negative zeta potential. Table 1 indeed reveals that the zeta potential of cubosomes decreased by 0.9 mV in the presence of PP50. The change has the expected sign but was small in magnitude. We, therefore, doubt that PP50 covered the particle surface extensively. The most likely scenario was that PP50 penetrated into the cubic phase water channels. The PP50 sample used in the present study has a number average mass of M_n = 23.0 kDa, while the segment represented in Figure 2 b has a molar mass of 700 Da, with an estimated length of 30 Å for a diameter of 14 Å (using a molecular model). Taking b = 30 Å as the Kuhn segment length of the repeat units, the polymer consisting of 33 segments has a gyration radius $R_g = \sqrt{33} / \sqrt{6}\, b$ = 70 Å. On the other hand, the water channel radius, r_w, can be estimated using the relation between r_w and the lattice parameter a:[40]

$$r_w = 0.305a - l \qquad (2)$$

with a = 163 Å and l = 18 Å one finds r_w = 32 Å. Mobility and penetration of PP50 chains in the cubic nanostructure therefore seems a reasonable assumption[41]. The magnitude of the cell size variation, the uniformity of the structures, the lack of sensitivity to particle dilution and the relative size of the polymer and the cubic cell make of the penetration of PP50 into the cubosome particles the most likely possibility.

We discuss now the possible mechanisms for the cell size increase in the presence of the polymer. We observed first that pH reduction only marginally decreased the measured unit cell size of the reference samples by 6 Å. By comparison, the addition of PP50 at pH 7.5 increased this value by 20 Å. The change of electric charge on the polymer backbone when decreasing pH from 7.5 to 5.5 did not seem to be a prominent factor. The measured lattice parameter at pH 5.5 in the absence and presence of PP50 were 137 and 167 Å respectively. This suggests that electrostatic repulsion is not a likely candidate for explaining the observed swelling. Moreover, all experiments were done under buffered conditions, in which electrostatic interactions were strongly screened. At pH 7.5 it is unlikely that the polymer inserts deeply into the bilayer. Modifications are probably therefore induced by the interaction between the water-soluble polymer and the monoolein interface. For instance, changes in the structure and a decrease in the parameter size of cubic phases exposed to polysaccharides were reported by Mezzenga *et al.*[42]. Whether the polymer is depleted or adsorbed by the membrane, its presence between the bicontinuous channels changes the free-energy at two levels. First, it induces direct interactions between different parts of the bilayer over the range of the polymer size. Secondly, the polymer-membrane interaction changes the curvature elastic constants of the bilayer, the bending rigidity κ and the Gaussian rigidity $\overline{\kappa}$. For depletion and equilibrium adsorption this is expected to decrease κ and increase $\overline{\kappa}$, while for inserted polymers, an increase in κ and a decrease in $\overline{\kappa}$ are expected.[43]

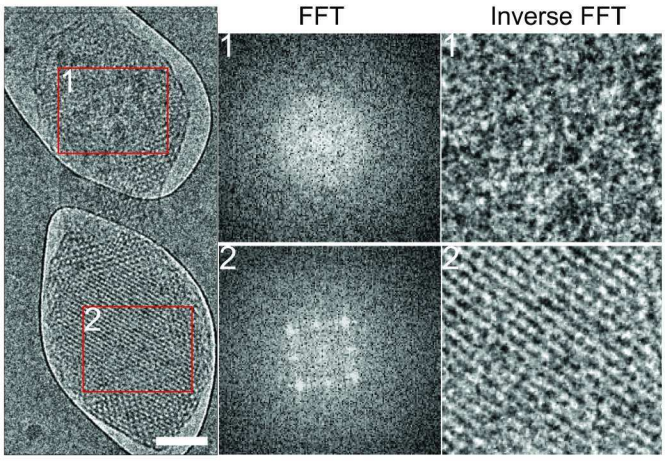

Fig. 5 Cryo-TEM images of a single cubosome at pH 5.5 with incorporated polymer. The red boxes represent the areas used for FFT calculations. Scale bar, 100 nm. (a = 156.0 Å). 1) upper part of particle; 2) lower part of particle.

The observed swelling of the cubosomes at pH 7.5 suggests that the presence of PP50 promoted a reduction in the magnitude of the spontaneous monolayer curvature. Hence, the spontaneous curvature of the lipid bilayer towards the water region decreased, resulting in a higher water uptake capacity.

Table 2 lists the variation of the lattice parameter a, measured by SAXS, the size of water pores r_w and the water volume fractions Φ_w. As can be observed, the water channel size increased while some polymer was incorporated into the cubic phase. At physiological pH, this suggests that the polymer behaved like a hydration-modulating agent i.e. favoured the hydration of the *Im3m* phase without changing the structure (Fig. 3 c,d). Similar swelling behaviour of cubic phases upon addition of additives has been reported previously by Angelov[44] and Negrini *et al.*[20]

Polymer-induced structural changes under acidic pH conditions

The well-resolved diffraction peaks obtained in SAXS (Fig. 3 a,b,c) at pH 7.5 or pH 5.5 without PP50 indicate well-ordered cubic phases. The Cryo-TEM images of a selection of particles show cubic ordering established across the whole particles. FFT image analysis displays characteristic fourfold symmetric patterns depending on the orientation of the particles with respect to the electron beam (Fig. 4 a,b,c,d). We conclude that the reference sample and the polymer loaded sample at pH 7.5 are composed of crystalline pieces of *Im3m* bicontinuous cubic phase.

Figure 4 e,f and Figure 5 show a selection of nanoparticles with PP50 at pH 5.5. We could see large disordered regions, with no visible periodic ordering, confirmed by the absence of peaks in the FFT image analysis. Disordered and cubic ordered regions coexisted, sometimes within the same particle. Fig. 5 shows a single particle in the same field of view: the upper part of the particle was mostly disordered, while the bottom of the particle still pre-

View Article Online
DOI: 10.1039/C7SM01620D

sented a cubic ordering. The particle in Fig. 4 f displayed some apparent lamellar order, associated with two spots in its FFT pattern. Therefore, cubosomes with polymer in acidic conditions can be seen as a collection of totally or partially disordered particles coexisting with cubic and lamellar ordered particles. The image analysis performed on the lamellar regions leads to a repeat distance comprised between 65 and 75 Å. The TEM observations account well for the observed SAXS patterns. Indeed, with only a small fraction of the particles retaining their cubic order, the *Im3m* diffraction peaks are faint in Fig. 4 d. The observed peak at q^* is consistent with a lamellar phase with a repeat distance $d =$ 50 Å rather different from the lamellar periodicity estimated by Cryo-TEM. This discrepancy might be due to a slow time evolution of the cubosome structure interacting with the hydrophobic polymer. The SAXS and the Cryo-TEM measured values could correspond to different ageing stages of the samples. We discussed here the effect of 10 wt% PP50, a compromise between the efficiency of the action and the required amount of polymer, preliminary results from smaller or larger concentrations show as expected corresponding trends.

4 Conclusions

We prepared pH-sensitive cubosomes from monoolein. Besides the monoglyceride, cubosomes contained Pluronic F127, a standard non-ionic surfactant and PP50, a pH-sensitive pseudopeptide. As expected, F127 swelled the liquid crystal, introducing a primitive cubic phase while stabilizing the monoolein cubic phase particles. Cubosomes without PP50 were not prone to disruption under acidic conditions at pH 5.5. Lipid particles with added PP50 were successfully disrupted when exposed to acidic conditions, paving the way for applications in drug delivery.

Conflict of interest

There are no conflicts to declare.

Acknowledgements

M. Kluzek, F. Thalmann, C.M. Marques, S. Wang, R. Chen, J. M. Seddon and M. Schmutz all acknowledge funding from the European FP7-MSCA International Training Network (ITN) SNAL 608184 (Smart Nano-objects for Alteration of Lipid-bilayers) to support the work. We thank Diamond Light Source (UK) for provision of x-ray beamtime (SM14217), Dr Andy Smith for his support and assistance and Dr Olga Shebanova for her assistance in using beamline I22. Cryo-TEM images were obtained using the ISO9001 Electron Microscopy platform at ICS Strasbourg.

References

1 P. Mariani, V. Luzzati and H. Delacroix. *Journal of Molecular Biology*, **204** (1), 165–189, 1988.

2 V. Luzzati, A. Tardieu, T. Gulik-Krzywicki, E. Rivas, and F. Reiss-Husson. *Nature*, **220** (5166), 485–8, 1968.

3 K. Larsson. *Nature*, **304** (5927), 664–664, 1983.

4 K. Larsson. *Current Opinion in Colloid and Interface Science*, **5** (1-2), 64–69, 2000.

5 H. T. McMahon and J. L. Gallop. *Nature*, **438** (7068), 590–596, 2005.

6 X. Mulet, B. J. Boyd and C. J. Drummond. *Journal of Colloid and Interface Science*, **393**, 1–20, 2013.

7 B. J. Boyd, D. V. Whittaker, S.-M. Khoo and G. Davey. *International Journal of Pharmaceutics*, **309** (1-2), 218–226, 2006.

8 S. Engstrom. *Lipid Technology*, 2, 42–45, 1990.

9 M. Nasr, M. K. Ghorab and A. Abdelazem. *Acta Pharmaceutica Sinica B*, **5** (1), 79–88, 2015.

10 J. C. Shah, Y. Sadhale and D. Chilukuri. *Advanced Drug Delivery Reviews*, **47** (2-3), 229–250, 2001.

11 K. Larsson. *Current Opinion in Colloid and Interface Science*, **14** (1), 16–20, 2009.

12 A.-Y. Idit, D. Libster, A. Aserin and N. Garti. *Current Opinion in Colloid and Interface Science*, **14** (1), 21–32, 2009.

13 C. J. Drummond and C. Fong. *Current Opinion in Colloid and Interface Science*, **4** (6), 449–456, 1999.

14 W.-K. Fong, Nino Malic, R. A. Evans, A. Hawley, B. J. Boyd and T. L. Hanley. *Biointerphases*, **7** (1-4), 1–5, 2012.

15 M. L. Lynch, A. Ofori-Boateng, A. Hippe, K. Kochvar and P. T. Spicer. *Journal of Colloid and Interface Science*, **260** (2), 404–413, 2003.

16 J. Clogston, G. Craciun, D.J. Hart and M. Caffrey. *Journal of Control Release*, **102** (2), 441–461, 2005.

17 R. Negrini, W.-K. Fong, B. J. Boyd and R. Mezzenga. *Chem. Commun.*, **51** (30), 6671–4, 2015.

18 E. Nazaruk, M. Szlęzak, E. Górecka, R. Bilewicz, Y. M. Osornio, P. Uebelhart, and E. M. Landau. *Langmuir*, **30** (5), 1383–90, 2014.

19 B. Angelov, A. Angelova, V. M. Garamus, G. Lebas, S. Lesieur, M. Ollivon, S. S. Funari, R. Willumeit and P. Couvreur. *J. Am. Chem. Soc.*, **129** (44), 13474–13479, 2007.

20 R. Negrini and R. Mezzenga. *Langmuir*, **28** (47), 16455–16462, 2012.

21 R. Negrini, A. Sanchez-Ferrer and Raffaele Mezzenga. *Langmuir*, **30** (15), 4280–4288, 2014.

22 Y. Aota-Nakano, S. J. Li and M. Yamazaki. *Biochimica et Biophysica Acta (BBA) - Biomembranes*, **1461** (1), 96 – 102, 1999.

23 Y. Okamoto, S. M. Masum, H. Miyazawa and M. Yamazaki. *Langmuir*, **24** (7), 3400–3406, 2008.

24 R. Negrini and R. Mezzenga. *Langmuir*, **27** (9), 5296–5303, 2011.

25 T. Oka, T. Saiki, J. M. Alam and M. Yamazaki. *Langmuir*, **32** (5), 1327–1337, 2016.

26 V. Ho, N. Slater and R. Chen. *Biomaterials*, **32** (11), 2953–2958, 2011.

27 R. Chen, S. Khormaee, M. E. Eccleston, and N. Slater. *Biomaterials*, **30** (10), 1954–1961, 2009.

28 S. Zhang, A. Nelson, Z. Coldrick and R. Chen. *Langmuir*, **27** (13), 8530–9, 2011.

29 A. L. Lynch, R. Chen, P. J. Dominowski, E. Y. Shalaev, R. J. Yancey Jr. and N. K. H. Slater. *Biomaterials*, **31**, 6096–6103, 2010.

30 A. L. Lynch, R. Chen and N. K. H. Slater. *Biomaterials*, **32**, 4443–4449, 2011.

View Article Online
DOI: 10.1039/C7SM01620D

31 J. Y .T. Chong, X. Mulet, L. J. Waddington, B. J. Boyd and C. J. Drummond. *Soft Matter*, **7** (10), 4768–4777, 2011.

32 R. Chen, M. E. Eccleston, Z. Yue and N. K. H. Slater. *J. Mater. Chem.*, **19** (24), 4217–4224, 2009.

33 T. Landh. *Journal of Physical Chemistry*, **98** (34), 8453–8467, 1994.

34 J. M. Seddon, A. M. Squires, C. E. Conn, O. Ces, A. J. Heron, X. Mulet, G. C. Shearman and R. H. Templer. *Philosophical Transactions of the Royal Society of London A, Mathematical, Physical and Engineering Sciences*, **364** (1847), 2635–2655, 2006.

35 A. Falchi, A. Rosa, A. Atzeri, A. Incani, S. Lampis, V. Meli, C. Caltagirone and S. Murgia. *Toxicology Research*, **4** (4), 1025–1036, 2015.

36 G. Popescu, J. Barauskas, T. Nylander and F. Tiberg. *Langmuir*, **23** (2), 496–503, 2007.

37 J. Gustafsson, H. Ljusberg-Wahren and M. Almgren. *Langmuir*, **12** (20), 4611–4613, 1996.

38 P. Garstecki and R. Hołyst. *Langmuir*, **18** (7), 2519–2528, 2002.

39 D. C. Turner, Z.-G. Wang, S. M. Gruner, D. A. Mannock, and R. N. McElhaney *J. Phys. II France*, **2** (11), 2039–2063, 1992.

40 J. Briggs, H. Chung and M. Caffrey. *J. Phys. II France*, **6** (5), 723–751, 1996.

41 R. Ghambari, S. Assenza, A. Saha and R. Mezzenga. *Langmuir*, **33** (14), 3491–3498, 2017.

42 R. Mezzenga, M. Grigorov, Z. Zhang, C. Servais, L. Sagalowicz, A. I. Romoscanu, V. Khanna and C. Meyer. *Langmuir*, **21** (14), 6165–6169, 2005.

43 T. Bickel and C. M. Marques. *Journal of Nanoscience and Nanotechnology*, **6** (8), 2386–2395(10), 2006.

44 B. Angelov, A. Angelova, Michel Ollivon, C. Bourgaux and A. Campitelli. *J Am Chem Soc.*, **125** (24), 7188–9, 2003.

View Article Online
DOI: 10.1039/C7SM01620D

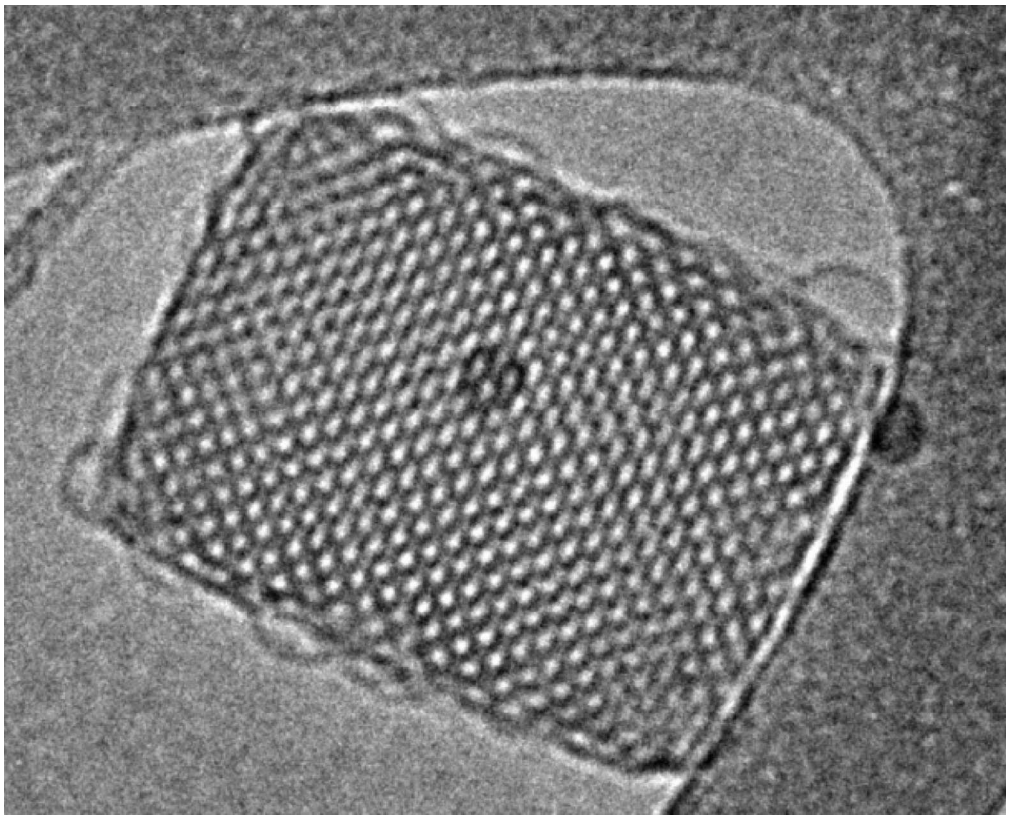

Graphical Abstract: Monoolein based cubosome nanoparticles incubated with a pH sensitive polymer are shown to be significantly altered under acidic conditions.

106x86mm (300 x 300 DPI)